Cement and Concrete Research 38 (2008) 1130–1134

Contents lists available at ScienceDirect

Cement and Concrete Research

journal homepage: http://ees.elsevier.com/CEMCON/default.asp

Discussion

A reply to the discussion "does C–S–H particle shape matter?" F.-J. Ulm and H. Jennings of the paper "modelling elasticity of a hydrating cement paste", CCR 37 (2007)

Julien Sanahuja [a,b,*], Luc Dormieux [b], Gilles Chanvillard [a]

[a] Lafarge Centre de Recherche, France
[b] École Nationale des Ponts et Chaussées, France

The question of the influence of the morphology of heterogeneous materials on their effective properties continues to be a formidable one, especially when this morphology is genuinely complex, as in cementitious materials. In fact, behind this question, we can identify two issues:

- Can the morphology be accurately described?
- Can a simplified (modelled) representation of the morphology be established to properly predict the effective properties of the material especially over a range of porosities which is relevant from a practical point of view?

As the microstructure of cement-based materials is very complex in nature, it is not so easy to decouple the effects of every parameter. Thus, we first focus on a hydrated composite showing a much clearer morphology, even if at a much larger scale:[1] gypsum. In the following, we would like to address whether the shape of the particles is a second order parameter with respect to the porosity as far as the effective stiffness is concerned, referring to both experimental and theoretical (numerical and semi-analytical) results. Then, in a second step, we go back to cementitious materials, starting with the effective properties of pure C–S–H.

1. Does particle shape of hydrated composites matter? An example from gypsum

The first question we would like to address is whether the influence of the particle shape on the mechanical properties of hydrated composites is negligible or not. These materials are porous polycrystals, made up of solid particles and pores. The effective mechanical properties of such materials depend on the behavior of the particles themselves and on the morphology, that is the geometrical distribution of the solid phase and the porous domain. To describe the morphology in a simplified way, at least two parameters are relevant: the porosity φ_0 (or the packing density $\eta_0 = 1 - \varphi_0$), and the shape of the particles. The question is whether the shape is a second order parameter with respect to the porosity, as far as effective mechanical properties are concerned.

When the packing density is relatively high ($\eta_0 > 0.6$), as the authors of the discussion point out, the shape of the particles clearly has a negligible influence (see Fig. 4 in F.-J. Ulm and H. Jennings discussion). We confirm this, adding another hydrated composite to the set of materials represented on this last figure: gypsum. This quite common material is made up of elongated and interlocked gypsum crystals (see Fig. 1). On Fig. 2, we plot experimental measurements of the normalized Young's modulus of gypsum samples (prepared avoiding the entrapment of air bubbles) as a function of the packing density, when this last parameter is above 0.6. The data points lie remarkably close to the linear scaling which comes from a self-consistent scheme with spherical solid particles (aspect ratio $r^s = 1$, Poisson's ratio $\nu^s = 0.2$). Thus, gypsum is a hydrated composite which seems to behave like the other ones dealt with on Fig. 4 of the discussion: the influence of the particle shape seems to be negligible, as the linear scaling $(2\eta_0 - 1)$ is able to describe the experimental data. From a theoretical point of view, this point had also been observed by Fritsch et al. [4]. This is true as long as we refrain from exploring packing densities outside the range $0.6 < \eta_0 < 1$.

Indeed, as far as lower packing densities are concerned, the experimental data points clearly deviate from the linear scaling (see Fig. 3). At $\eta_0 = 0.4$, the effective stiffness is still around 10% of the one of the solid crystals. Such a departure from the $(2\eta_0 - 1)$ linear scaling reveals that the effective stiffness of gypsum cannot be estimated resorting to a self-consistent scheme with spherical particles, considering the whole range of packing densities of interest. Thus, even if featuring crystals much larger than the C–S–H particles, the gypsum material seems to be in contradiction with the last paragraph of F.-J. Ulm and H. Jennings discussion. The authors argue that as precipitation and growth of particles are random, the contact surfaces are randomly oriented. We agree on this. But then the effective stiffness of gypsum cannot be properly modelled neglecting the fact that the crystals are needle-shaped, even if the contact surfaces are randomly oriented.

Note that gypsum is not the only porous polycrystal to exhibit non zero stiffness at a packing density below 0.5. Hydroxyapatite-based biomaterials also show up this trend, as shown in Fig. 25.7, page 547 in the book [5]. Among the experimental results plotted on this figure, materials with a packing density between 0.45 and 0.5 and a Young's modulus between 10 and 20 GPa can be found. In this book chapter, the authors model hydroxyapatite-based biomaterials resorting to needle-shaped solid particles.

* Corresponding author. Lafarge Centre de Recherche, France.
E-mail address: julien.sanahuja@lafarge.com.

[1] As far as modelling is concerned, as we are using Eshelby-based homogenization of random media, the results do not depend on the size of the particles, but on morphological parameters such as the porosity and the shape of the particles.

0008-8846/$ – see front matter
doi:10.1016/j.cemconres.2008.03.024

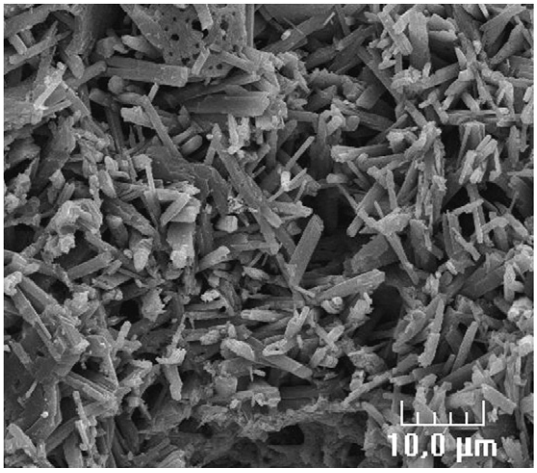

Fig. 1. SEM image of gypsum, which reveals elongated and interlocked crystals.

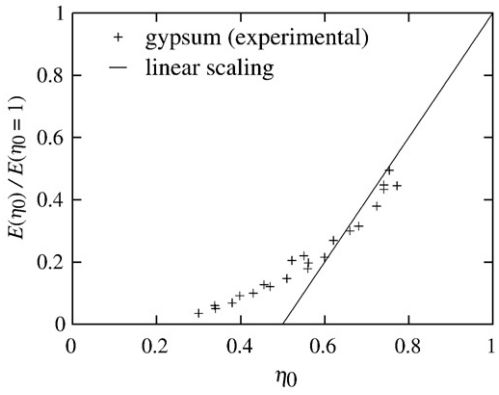

Fig. 3. Normalized stiffness vs. packing density, experimentally measured on gypsum samples (data from [1,2,8,10,13]), and linear scaling ($2\eta_0-1$).

The fact that the particles shape is not a second order parameter should not be a problem from the modelling point of view. For example, numerical FEM approaches [11] or homogenization schemes [14] are readily available to deal with the influence of both the packing density and the aspect ratio of the particles. Interestingly, these two micro-to-macro techniques, although fundamentally different from a theoretical point of view, yield very close results on both the Young's modulus E and the Poisson's ratio ν (see Fig. 4). Note that the self-consistent scheme with spherical particles ($r^s=1$, results plotted using a dotted line on Fig. 4) is unable to reproduce properly the numerical FEM computations as soon as $\eta_0<0.7$.

2. And what about C–S–H?

The previous section pointed out that gypsum exhibits non negligible effective stiffness for packing densities much lower than 0.5. The question we want to address now is whether this pattern also shows up on C–S–H. According to the authors of the discussion (see the right part of Fig. 2 and text at the beginning of paragraph " C–S–H density, nanoindentation modulus and hardness and sans results"), C–S–H exhibit a critical packing density of 0.5 under which elasticity and strength vanish. We would be more prudent on this, as we think that drawing conclusions on the whole range of packing densities, and especially on the critical packing density would require more experimental points. Also the model relations between the indentation hardness and the packing density plotted on Figs. 2(c) and 3(b) are different (line vs. curve), which seems to be a little misleading.

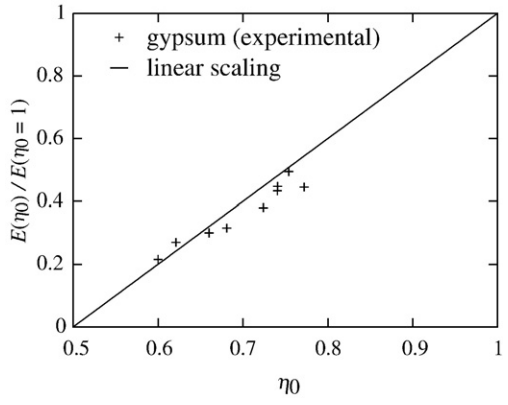

Fig. 2. Normalized Young's modulus vs. packing density, experimentally measured on gypsum samples (subset of data from [1,2,8,10], limited to the range $0.6<\eta_0<1$), and linear scaling ($2\eta_0-1$).

It thus seems interesting to take advantage of Feldman and Beaudoin [3] experiments on 14 Å tobermorite compacts (a crystalline version of C–S–H, often referred to as a model of C–S–H). They measured a packing density of 0.4 and a Young's modulus of 2 GPa, which is far from negligible. As the packing density is lower than 0.5, this suggests that the shape of the solid particles to be used in the model should depart from the sphere. As a straightforward application of the micromechanical model developed and validated in Section 2.2.1 of our paper, we can estimate the particles aspect ratio required to get a Young's modulus of 2 GPa with a packing density of 0.4. Using the solid stiffness given in Table 3 of our paper, the calculated aspect ratio is 0.16. Moreover, some experimental evidence seems to support this non spherical shape, required as far as modelling is concerned: see [6], who identified, by AFM, elementary bricks measuring 60*30*5 nm. The aspect ratio of these bricks can be estimated as $5/\sqrt{30*60}\approx 0.12$, which is remarkably close to the value 0.16 previously calculated. Also, in [9], Jennings proposes a new model for its globules making up the C–S–H gel, introducing brick-like particles instead of spheres.

As the authors of the discussion do, one may argue that the stiffness of the solid particles (characterized by the Young's modulus $E^s=71.6$ GPa) is unrealistic compared to atomistic simulation results. Recent computations done by Pellenq [12] on 14 Å tobermorite, at $C/S=0.83$ and at its maximum of stability, show Young's moduli of 54 GPa perpendicular to the sheets plane, and 68 and 72 GPa in the two directions along the sheets plane. Our estimation by reverse analysis, $E^s=71.6$ GPa (see the last paragraph of Section 2.3.2 in our paper), is of the same order of magnitude, albeit a little higher. Nevertheless, a lower value of the solid Young's modulus yields, according to the computation referred to in the previous paragraph, slightly flatter solid particles. For example, when $E^s=55$ GPa (compared to 71.6 GPa), the estimated aspect ratio is 0.15 (instead of 0.16), which comes even closer to the aspect ratio 0.12 of the elementary bricks.

Going back to the interpretation of the frequency distribution of nano-indentation measurements, the authors of the discussion conclude for ultra-high density C–S–H phase. We think this is a bit premature without confirming that the high stiffness or hardness found is not a result of interactions with residual anhydrous phases. Further investigation should be performed to clarify this point.

3. Back to cement pastes

For illustrative purposes, simulations can be performed using the micromechanical model proposed in Section 2 of our paper, modifying *only one* parameter: the aspect ratio of the particles making up the outer matrix. We consider successively platelet-like (oblates, as done in the paper), needle-like (prolates), and spherical particles.

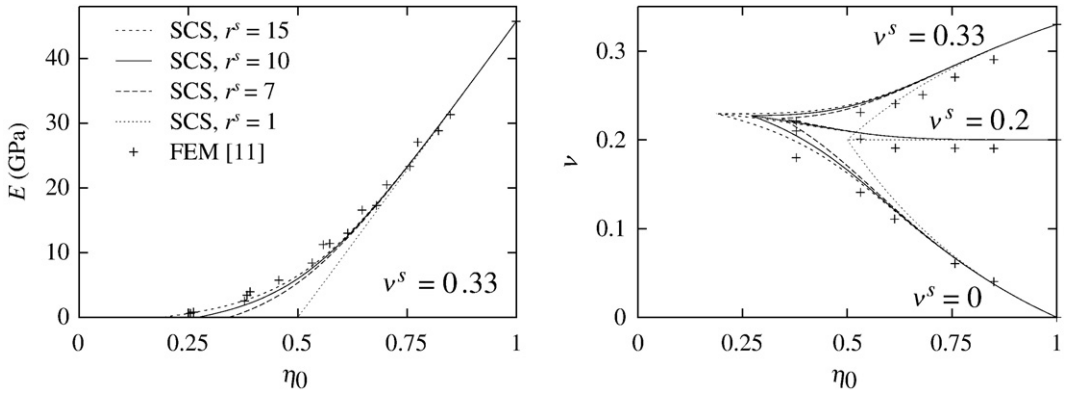

Fig. 4. Young's modulus and Poisson's ratio numerically computed (FEM, from [11]), and estimated by a self-consistent scheme (SCS, from [14]) involving elongated solid particles of aspect ratio r^s: the Young's modulus E has been calculated with a solid phase characterized by the Young's modulus E^s=46 GPa and the Poisson's ratio ν^s=0.33; the Poisson's ratio ν has been calculated from three different values of the solid Poisson's ratio, namely ν^s=0, 0.2 and 0.33 (see the end of the curves, at η_0=1).

The aspect ratio of the prolates has been calibrated as described in Section 3.1 of the paper: this yields r^s=19.

On the right part of Fig. 5, the effective Young's modulus of the paste is plotted vs. the degree of hydration, as modelled resorting to the three particle shapes, and experimentally measured. Two w/c ratios are considered: 0.3 and 0.5. To help the analysis of these curves, the packing density of the outer hydrates (as estimated by the hydration model described in Section 2.3.1 of our paper) is plotted as a function of the degree of hydration on the left part of Fig. 5. Indeed, in the micromechanical model proposed in Section 2 of our paper, the setting of the paste occurs when the outer hydrates (matrix of the paste) become solid, that is when their packing density reaches the critical packing density corresponding to the shape of the particles (see Fig. 6 of our paper).

Note that the spherical shape gives the worst results. The critical packing density η_0^c=0.5 associated with the spherical shape is clearly too high: the degree of hydration required to reach such a critical packing density in the outer hydrates is unreasonably high (see left part of Fig. 5). With either platelets or needles, this critical packing density drops considerably (depending on the aspect ratio of the

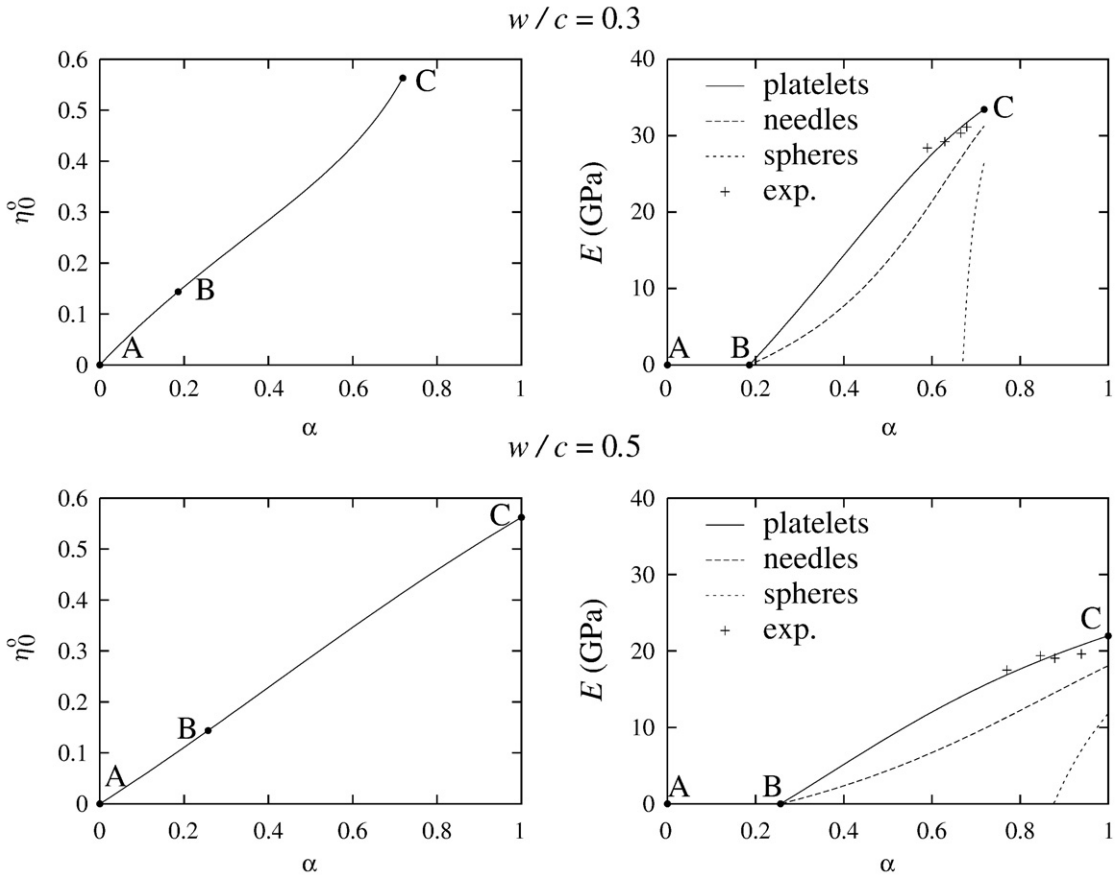

Fig. 5. Left part: packing density of the outer hydrates vs. degree of hydration; Right part: Young's modulus vs. degree of hydration estimated by model developed in Section 2 of the paper, considering platelet-like, spherical and needle-like solid particles in outer C–S–H, and experimental measurements from [7]; pastes characterized by w/c=0.3 and 0.5.

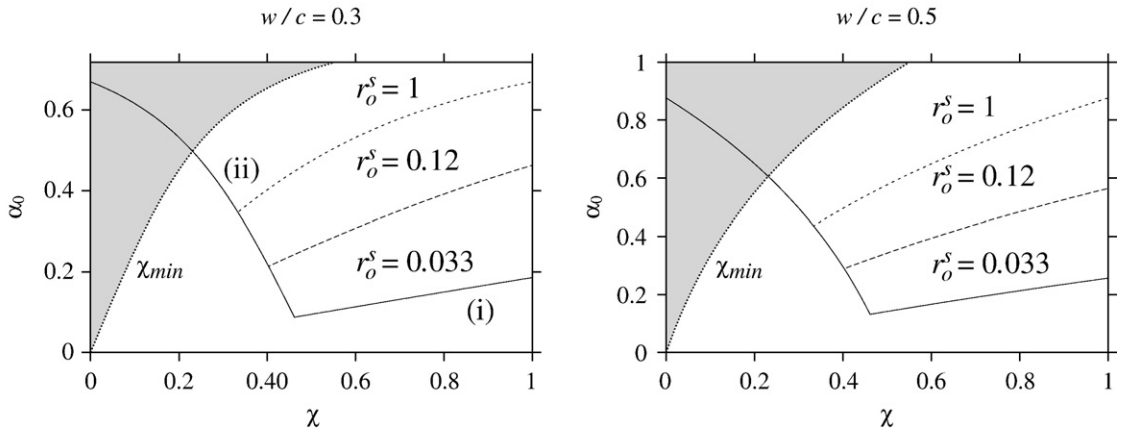

Fig. 6. Degree of hydration at setting vs. volume fraction χ of small pores in the pore space of the matrix, for w/c=0.3 and 0.5, and the particles aspect ratios r_o^s=*0.033, 0.12 and 1; only the part of the graph situated on the right of the dotted line is valid* ($\chi > \chi_{min}$).

particles: see Fig. 6 of our paper), which allows setting at a more reasonable degree of hydration. Compared to the needle shape, the platelet shape is found to provide Young's modulus estimates which are closer to the experimental measurements. Consequently, we have to conclude that the platelet shape seems to be the most suited to properly describe the experimental results.

We should mention that the model proposed in our paper is aimed at estimating the stiffness of the cement paste as hydration proceeds, from the beginning to the very end. To this respect, three points are defined on the curves corresponding to platelets: A at α=0, B at setting and C at the end of hydration. From A to B, the packing density of the outer hydrates has not yet reached the critical packing density associated to the shape of the particles. In other words, the amount of solid hydrates precipitated into the initially water-filled space is not enough to achieve a solid material. From B to C, the packing density of the outer hydrates still increases as more and more particles precipitate. As the critical packing density is now exceeded, the stiffness of the outer matrix increases. The stiffness of the paste also increases.

As the packing density of the outer hydrates grows during hydration, it is not surprising to find that the shape of the particles has less influence near the end of hydration (see point C where $\eta_0^o \approx 0.6$). However, as far as the beginning of hydration is concerned, the shape of the particles is found to be of paramount importance (compare the curves plotted on Fig. 5 for platelets and spheres).

Also, we experienced some difficulties to properly analyse the Fig. 2 of the discussion. Indeed, this figure seems to compare two relations at fundamentally different scales:

- indentation modulus or hardness of C–S–H vs. theoretical packing density of C–S–H,
- strength of cement paste vs. capillary porosity of paste.

The figure suggests that the same linear scaling starting at a porosity of 0.5 is relevant to model both relations. This seems to be a little misleading since pastes are not made up of pure C–S–H, and the capillary porosity of a paste (volume of capillary pores/volume of paste) can hardly be compared to the C–S–H porosity (volume of gel pores/volume of C–S–H). For example, at lower w/c, part of the cement grains remain unhydrated even in mature pastes. Moreover, the capillary porosity, as defined in [15] (closely linked to capillary water), does not include the gel pores of hydrates.

Speaking of capillary pores, one may argue that not explicitly taking them into account in the matrix surrounding the composite spheres (anhydrous+inner) leads to a too uniform distribution of the solid particles making up this matrix at the lower scale. A less uniform distribution of the solid phase, leaving large empty spaces as capillary pores, would certainly allow similar degrees of hydration at setting with less flat solid particles. Taking into account the existence of the capillary pores is precisely the purpose of the Section 3.5 of our paper (compare Fig. 4 and 17). A new morphological parameter is introduced: the volume ratio χ of small (that is, non capillary) pores with respect to the whole pore space of the matrix. Unfortunately, much further investigation is necessary to clarify the way χ depends on w/c and α. Nevertheless, we can keep χ as a parameter and see if we can draw interesting conclusions on the degree of hydration at setting without more precisions on this parameter. On Fig. 6, the degree of hydration at setting is plotted as a function of χ for some values of w/c and of the aspect ratio r_o^s of the outer particles. It is basically the Fig. 18 of our paper (see Section 3.5 for further details), where we have added the curve corresponding to spherical particles (r_o^s=1). The minimal setting degree of hydration that spherical particles allow is α_0^{min}=0.34 at w/c=0.3 and α_0^{min}=0.44 at w/c=0.5. In fact, the degree of hydration at setting, predicted with spherical particles, is too high, whatever the value of χ. Therefore, we have to conclude that a model based on spherical C–S–H solid particles cannot estimate properly the onset of the stiffness of a cement paste.

4. Conclusion

Only in porous polycrystals showing a relatively high packing density ($\eta_0 > 0.6$), the shape of the particles is a parameter of second order with respect to the porosity when determining the effective stiffness. Enough evidence has been gathered to support this point, experimentally [1,2,8,10] (see Fig. 4 of the discussion and Fig. 2), numerically by FEM [11] (see Fig. 4), and from a homogenization scheme [14] (see Fig. 4). However, a great deal of experimental evidence (see [1,2,8,10,13] on gypsum, [5] on hydroxyapatite-based biomaterials, [3] on tobermorite) indicates that the porosity 0.5 is not a critical value in general. Hydrated composites can be commonly encountered at lower packing densities, especially during hydration. In particular, theoretical modelling of setting of cement pastes seems to be strongly coupled with shape effects.

To conclude, while the $(2\eta_0 - 1)$ linear scaling is found to be relevant to model the stiffness of porous polycrystals in the range $0.6 < \eta_0 < 1$ of packing densities, both experimental and modelling evidence seem to support that this convenient relation should, by far, not be applied to every material at every scale.

Acknowledgements

The authors gratefully acknowledge J. Chen, E. Guillon and B. Zuber for fruitful discussions, comments and suggestions.

References

[1] M.A. Ali, B. Singh, The effect of porosity on the properties of glass fibre-reinforced gypsum plaster, Journal of Materials Science 10 (1975) 1920–1928.
[2] A. Colak, Physical and mechanical properties of polymer-plaster composites, Materials Letters 60 (16) (2006) 1977–1982.
[3] R.F. Feldman, J.J. Beaudoin, Microstructure and strength of hydrated cement, Cement and Concrete Research 6 (3) (1976) 389–400.
[4] A. Fritsch, L. Dormieux, C. Hellmich, Porous polycristals built up by uniformly and axisymmetrically oriented needles: homogenization of elastic properties, Comptes Rendus Mecanique 334 (2006) 151–157.
[5] A. Fritsch, L. Dormieux, C. Hellmich, J. Sanahuja, in: A.R. Boccaccini, J.E. Gough (Eds.), Tissue engineering using ceramics and polymers, chapter Micromechanics of hydroxyapatite-based biomaterials and tissue engineering scaffolds, Woodhead, 2007, pp. 529–565.
[6] S. Garrault, E. Finot, E. Lesniewska, A. Nonat, Study of C–S–H growth on C_3S surface during its early hydration, Materials and Structures 38 (2005) 435–442.
[7] C.-J. Haecker, E.J. Garboczi, J.W. Bullard, R.B. Bohn, Z. Sun, S.P. Shah, T. Voigt, Modeling the linear elastic properties of Portland cement paste, Cement and Concrete Research 35 (2005) 1948–1960.
[8] E.I. Tazawa, Effect of self stress on flexural strength of gypsum-polymer composites, Advanced Cement Based Materials 7 (1998) 1–7.
[9] H.M. Jennings, Refinements to colloid model of C–S–H in cement: CM-II, Cement and Concrete Research 38 (2008) 275–289.
[10] S. Meille. Etude du comportement mécanique du plâtre pris en relation avec sa microstructure. PhD thesis, INSA Lyon, 2001.
[11] S. Meille, E.J. Garboczi, Linear elastic properties of 2D and 3D models of porous materials made from elongated objects, Modelling and Simulation in Materials Science and Engineering 9 (5) (2001) 371–390.
[12] R.J.-M. Pellenq. personal communication.
[13] K.K. Phani, Young's modulus-porosity relation in gypsum systems, American Ceramic Society bulletin 65 (12) (1986) 1584–1586.
[14] J. Sanahuja, L. Dormieux, G. Chanvillard, Modelling elasticity of a hydrating cement paste, Cement and Concrete Research 37 (2007) 1427–1439.
[15] G.J. Verbeck, R.H. Helmuth, Structures and physical properties of cement paste, 5th international symposium on chemistry of cement, vol. 3, Tokyo, 1968, pp. 1–44.